Nitric Oxide 62 (2017) 32–43

Contents lists available at ScienceDirect

Nitric Oxide

journal homepage: www.elsevier.com/locate/yniox

Melatonin influences NO/NOS pathway and reduces oxidative and nitrosative stress in a model of hypoxic-ischemic brain damage

Santos Blanco [a, *], Raquel Hernández [a], Gustavo Franchelli [a], Manuel Miguel Ramos-Álvarez [b], María Ángeles Peinado [a]

[a] Area of Cell Biology, Department of Experimental Biology, University of Jaén, Campus Las Lagunillas s/n, 23071, Jaén, Spain
[b] Area of Methodology of the Behavioural Sciences, Department of Psychology, University of Jaén, Campus Las Lagunillas s/n, 23071, Jaén, Spain

ARTICLE INFO

Article history:
Received 23 September 2016
Received in revised form
28 November 2016
Accepted 3 December 2016
Available online 8 December 2016

Keywords:
Melatonin
Nitric oxide
Ischemia
Hypobaric hypoxia
Antioxidant: oxidative and nitrosative stress

ABSTRACT

In this work, using a rat model combining ischemia and hypobaric hypoxia (IH), we evaluate the relationships between the antioxidant melatonin and the cerebral nitric oxide/nitric oxide synthase (NO/NOS) system seeking to ascertain whether melatonin exerts its antioxidant protective action by balancing this key pathway, which is highly involved in the cerebral oxidative and nitrosative damage underlying these pathologies.

The application of the IH model increases the expression of the three nitric oxide synthase (NOS) isoforms, as well as nitrogen oxide (NOx) levels and nitrotyrosine (n-Tyr) impacts on the cerebral cortex. However, melatonin administration before IH makes nNOS expression response earlier and stronger, but diminishes iNOS and n-Tyr expression, while both eNOS and NOx remain unchanged. These results were corroborated by nicotine adenine dinucleotide phosphate diaphorase (NADPH-d) staining, as indicative of *in situ* NOS activity. In addition, the rats previously treated with melatonin exhibited a reduction in the oxidative impact evaluated by thiobarbituric acid reactive substances (TBARS). Finally, IH also intensified glial fibrillary acidic protein (GFAP) expression, reduced hypoxia-inducible factor-1alpha (HIF-1α), but did not change nuclear factor kappa B (NF-κB); meanwhile, melatonin did not significantly affect any of these patterns after the application of the IH model.

The antioxidant melatonin acts on the NO/NOS system after IH injury balancing the release of NO, reducing peroxynitrite formation and protecting from nitrosative/oxidative damage. In addition, this paper raises questions concerning the classical role of some controversial molecules such as NO, which are of great consequence in the final fate of hypoxic neurons.

We conclude that melatonin protects the brain from hypoxic/ischemic-derived damage in the first steps of the ischemic cascade, influencing the NO/NOS pathway and reducing oxidative and nitrosative stress.

1. Introduction

Cerebral ischemic-hypoxic (IH) pathologies are among the leading causes of death and long-term disability in Western countries. The ischemic-hypoxic-insult itself, as well as the subsequent reoxygenation period, can lead to the generation of a great amount of reactive nitrogen and oxygen species (RNS and ROS, respectively). These free radicals affect many biological molecules, triggering diverse cellular pathways that induce neurodegenerative processes involving inflammation, glial reactivity and even neuronal death [1].

Many studies have evidenced the implication of nitric oxide (NO) in these IH processes within the Central Nervous System

Abbreviations: C, control; CNS, central nervous system; eNOS, endothelial nitric oxide synthase; GFAP, glial fibrillary acidic protein; HIF-1, hypoxia inducible factor 1; HRE, hypoxia-responsible element; IH, ischemia-hypoxia; IκB, nuclear factor kappa B inhibitor; iNOS, inducible nitric oxide synthase; Mel, melatonin; NADPH-d, NADPH-diaphorase; NF-κB, nuclear factor kappa B; NO, nitric oxide; NOS, nitric oxide synthase; nNOS, neuronal nitric oxide synthase; NOx, nitrogen oxides; n-Tyr, nitrotyrosine; $ONOO^-$, peroxynitrite; PHDs, prolyl hydroxylases; pVHL, von Hippel-Lindau protein; RNS, reactive nitrogen species; ROS, reactive oxygen species; TBARS, thiobarbituric acid reactive substances; VEGF-A, vascular endothelial growth factor A.

* Corresponding author. Department of Experimental Biology (Building B-3), University of Jaén, Campus Las Lagunillas s/n, 23071, Jaén, Spain.
E-mail addresses: sblanco@ujaen.es (S. Blanco), rhernand@ujaen.es (R. Hernández), r6.gustavo@gmail.com (G. Franchelli), mramos@ujaen.es (M.M. Ramos-Álvarez), apeinado@ujaen.es (M.Á. Peinado).

http://dx.doi.org/10.1016/j.niox.2016.12.001
1089-8603/

[2–6]. NO is produced by three different isoforms of nitric oxide synthases (NOS), which convert L-arginine to L-citrulline with the consequent release of NO: neuronal NOS (nNOS) and the endothelial form (eNOS) are modulated by Ca^{2+}activated calmodulin whereas the inducible isoform (iNOS) is calcium-independent.

The inflammatory processes that follow HI injury are closely related to the NO/NOS system balance. Particularly, glial reactivity, mediated by the glial fibrillary acidic protein (GFAP) in astrocytes [7], has been associated with the excitoxicity by glutamate-NO-cGMP pathway; this pathway leads to greater NO production and other factors [8], that in turn can participate in the regulation of the activity of the NOS isoforms during ischemia [9]. In this sense, the release of inflammatory cytokines from astrocytes and other glial cells may activate the nuclear factor kappa B/Inhibitor of κB (NF-κB/IκB) pathway in neurons, and thus the subsequent biosynthesis of iNOS that produces high quantities of NO in an unregulated fashion [3,10–12].

Moreover, NO can participate in the ischemic cascade through the regulation of the hypoxia-inducible factor (HIF-1) via S-nitrosation of Cys 800 [13,14]; in addition, it promotes the accumulation of functional HIF-1α in the cytoplasm [15,16] which in turn is translocated to the nucleus inducing the expression of a battery of genes, some closely related to the NO/NOS system and involved in the hypoxic response, too [17].

In this sense, after hypoxia, nNOS seems to be the first isoform involved in the neuronal damage [18,19], although more recent researches have also showed that nNOS protects neurons from ischemic damage [20]. There is greater agreement about the neurotoxic role of iNOS in these pathologies, because this isoform raises the levels of NO inducing IH damage [19]. Finally, eNOS seems to exert a neuroprotective effect following brain ischemia [21,22] although its role in this pathology has been questioned as well [23].

When NO is produced in large amounts, it can react with superoxide (O_2^-), which is also severely produced under hypoxic conditions. Both reactive species form the strong oxidant peroxynitrite ($ONOO^-$) [24–26]. One of the most negative effects of $ONOO^-$ is the nitration of tyrosine residues of proteins (n-Tyr), thereby altering protein structure and functionality, causing severe damage to other molecules in the cell [27]. Therefore, the regulatory balance in the production of NO and its derived species depends not only on the activity of the NOS isoforms but also on the oxidative state of the cell, both determining the cell fate after IH [28,29].

According to the foregoing, avoiding the excessive production of ROS would be a suitable strategy to decrease RNS and consequently, to counteract IH-derived damage. In this sense, an appropriate approach could involve pharmacological preconditioning through the administration of natural antioxidants, such as melatonin, a compound that protects tissues from oxidative stress neutralizing ROS and RNS, among many other functions [30–32]. In fact, the neuroprotective role of melatonin has been extensively demonstrated in neurodegenerative diseases such as Parkinson, Alzheimer, epilepsy, and even in ischemic injury [31,33–36]. It is also known that melatonin protects the ischemic brain against lipid peroxidation [37], prevents neuronal death in a wide variety of neurodegenerative models, and stimulates antioxidant enzymes [38]. The ability of melatonin to induce an antioxidant cascade enhances its efficiency against oxidative damage [39], although its neuroprotective action, particularly in relation to the neutralization of the RNS and its relationships with the NO/NOS system, is not yet fully understood.

In summary, during IH, high amounts of ROS and RNS are produced, with a subsequent surge in the expression of nitrated proteins and the induction of cell damage and apoptosis. Given the key role of the NO/NOS system in these events, we hypothesize that melatonin, a substance capable of reducing oxidative stress, could exert its neuroprotective effect after IH, as least in part, by modulating the NO/NOS system response. With this aim, we have analyzed the following parameters in brain cortical samples of Wistar rats submitted to an IH model with or without previous melatonin administration: 1) NO/NOS system balance (nNOS, eNOS, and iNOS expression; NADPH-diaphorase activity; and NOx levels); 2) glial reactivity (GFAP expression); 3) oxidative and nitrosative status of the tissue (TBARS determination and n-Tyr expression); and 4) elements involved in the molecular response to IH injury and highly related to the NO/NOS system (HIF-1α and NF-κB).

2. Methods

2.1. Animals

The study was performed on 60 adult male Wistar rats provided by Harlan Laboratories (Envigo) and weighing 350 g each, kept under standard conditions of light and temperature and allowed *ad libitum* access to food and water. The animals were assigned to six different groups: 1) C: control; 2) Mel + C: control treated with melatonin; 3) 0h: submitted to IH model and 0h of reoxygenation; 4) 0h + Mel: treated with melatonin, submitted to IH model and 0h of reoxygenation; 5) 2h: submitted to IH model and 2h of reoxygenation; 6) 2h + Mel: treated with melatonin, submitted to IH model and 2h of reoxygenation; for details see section 2.3. All procedures were performed in accordance with the EU Directive 2010/63/EU (2010), reviewed by the Ethics Committee of the Spanish Council for Scientific Research, approved by the Committee of Bioethics of the University of Jaén (Spain), and comply with the Uniform Requirements for manuscripts submitted to biomedical journals.

2.2. Melatonin administration

Melatonin (100 mg/kg body weight, Sigma, St. Louis, USA) diluted in saline and 2% methanol, Sigma, St. Louis, USA), or vehicle, were injected i.p. always at 8.30 a.m., 1 h prior to the onset of IH. The dose of melatonin (100 mg/kg body weight) was chosen according to similar works where the same dose was used [40–42].

2.3. Cerebral ischemic-hypoxic (IH) model

The rats were anesthetized with ketamine (100 mg/kg body weight, i.p.) and xylazine (5 mg/kg body weight, i.p.) 1h after antioxidant administration (Mel groups). Cerebral ischemia was induced by a modification of the Levine/Vannucci model, which basically consists of unilateral common carotid artery occlusion followed by a hypoxic stress for a predetermined time [43] and which has been successfully applied both to neonatal [44,45] and adult animals [46,47]. After isolation, ligation, and sectioning of left common carotid artery, the animals recovered for 2h and were submitted to hypobaric hypoxia (Fig. 1a). Body temperature was monitored and maintained throughout all the procedures. The sham animals submitted to surgery without vessel sectioning were used as the control group. Hypoxia was induced by down-regulating the environmental O_2 pressure to a final barometric pressure of approximately 300 hPa inside a hypobaric chamber. More specifically, hypobaric hypoxia was induced using a slight modification of a previously published procedure [48,49]. Briefly, the rats were placed in a hypobaric chamber in which the air pressure was controlled by means of a continuous vacuum pump and an adjustable inflow valve. The chamber was also provided

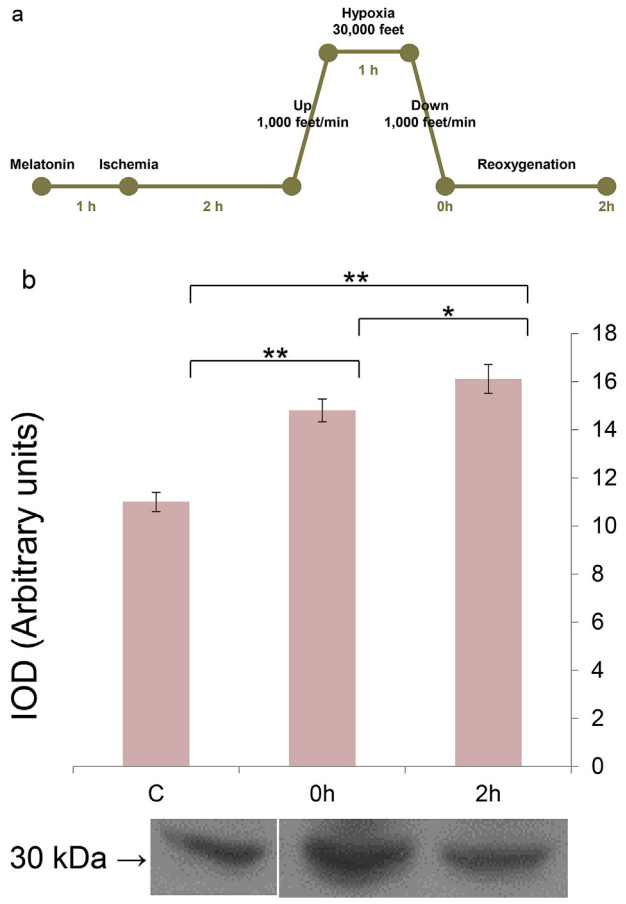

Fig. 1. a) Schematic representation of the experimental model used in this study. Briefly, melatonin was injected i.p. 1h prior to IH. Brain ischemia injury was induced by permanent occlusion of the left common carotid artery. Two hours after recovery, the rats were placed in a hypobaric chamber. Hypoxia was induced by down regulating the environmental O_2 pressure to an approximate final barometric pressure of 300 hPa. These conditions simulate an altitude of 9144 m (30,000 feet) and were maintained for 1h. The ascent/descent speed was kept below 300 m/min. After the period of hypoxia, animals were killed immediately (0h) or kept at atmospheric pressure for 2h. **b)** Western blot analysis of fractin in brain cortex cytosolic extracts of control (C) and IH (0h, 2h) rats. The amount of protein load per lane was 20 μg. Total protein amount of samples showed no differences between any experimental group and control; data (mean ± SEM) are expressed in mg/ml (C, 4.95 ± 0.13; 0h, 5.01 ± 0.12; 2h, 4.90 ± 0.15). Representative autoradiography of the corresponding fractin band is displayed in the bottom panel. The results are average values of five experimental animals in each group.

with a manometer to check the experimental altitude during the process. The conditions, simulating an altitude of 9144 m (30,000 feet), were maintained for 1 h. Ascent and descent rates were kept below 300 m/min (approximately 1000 feet/min). After the hypoxic period, the return to normobaric normoxic conditions spanned 30 min. The animals were either killed immediately after the hypobaric chamber was opened (0h and Mel+0h groups) or kept at atmospheric pressure under standard conditions of light and temperature and allowed *ad libitum* access to food and water for 2h and then killed (2h and Mel+2h groups) (Fig. 1a). Sham animals kept in the chamber under normobaric normoxic conditions served as controls (C and Mel + C groups). We have included the western blot study of the expression of the marker of apoptosis-related events fractin (Fig. 1b), which demonstrates apoptotic damage as consequence of the IH model.

2.4. Western blot analysis

After the corresponding reoxygenation times, the rats were killed by cervical dislocation, and the brain cortices of 5 rats from each group were dissected, rinsed in saline solution, frozen in liquid nitrogen, and stored at −80 °C until analyzed. Tissues were homogenized in 1/3 (w/v) of 30 mM Tris−HCl, pH 7.4, containing 0.5 mM DTT, 1 mM EDTA, 1% SDS, and protease inhibitor cocktail (Roche, Basel, Switzerland). The resulting homogenates were centrifuged for 1h at 100,000×*g*. All the procedures were performed at 4 °C. Protein concentrations in the supernatants were determined by the Bradford method [50]. Equal amounts (20 μg) of the denatured proteins were loaded per lane and separated on NuPAGE® Novex 4–12% Bis-Tris Gels (Invitrogen, Carlsbad, USA) as described by Laemmli [51]. Afterwards, proteins were transferred to a PVDF membrane using the XCell SureLock™ Mini-Cell system (Invitrogen, Carlsbad, CA, USA). The membranes were blocked with 2.5% powdered non-fat milk in 25 mM Tris-HCl, pH 7.6, 137 mM NaCl, 2.6 mM KCl, and 0.1% Tween 20 and incubated overnight at 4 °C with diluted rabbit polyclonal antibodies: anti-fractin (1:1,500, Chemicon Int., Temecula CA, USA), anti-nitrotyrosine (1:2,000, gift from J. Rodrigo of Instituto Cajal, Madrid, Spain), anti-nNOS (1:3,000, gift from V. Riveros-Moreno of Welcome Research Laboratories, Berkenhem, UK), and anti-GFAP (1:5,000, Dako, Glostrup, Denmark); and with mouse monoclonal antiserum anti-eNOS (1:800, Transduction, Lexington, KY, USA), and anti-iNOS (1:700, Transduction, Lexington, KY, USA) in blocking solution. All the antibodies used in this study have been previously tested by our group and others, showing specificity for their respective antigens [52,53]. Bound antibodies were revealed by means of an enhanced chemiluminescence kit (Amersham ECL Prime Western blotting detection reagent, GE Healthcare, Little Chalfont, UK) according to the manufacturer's instructions. The amount of proteins in each sample was quantified by densitometric scanning and expressed as arbitrary units (AU). The main proteins that are routinely used as loading control markers, β-actin, α-tubulin and GAPDH, were found to be altered in this model of OD (preliminary results of proteomic analysis not shown). Thus, we show the total protein data of the samples, instead of a loading control, in order to clarify the differences found in the western blot of the proteins analyzed were really due to abundance changes and not to variations in total protein content among any experimental group or controls.

2.5. Production of NO

NO production was determined by tissue accumulation of nitrite and nitrate in the brain cortex. Briefly, a portion of tissue from 5 animals of each group was homogenized in 3 vol (w/v) of PBS (pH 7.6) at 4 °C. Homogenates were then sonicated and centrifuged at 100,000×*g* for 60 min at 4 °C. The nitrate plus nitrite (NOx) was determined in the supernatants using a colorimetric kit according to the manufacturer's instructions (Nitrate/Nitrite colorimetric Assay Kit. Cayman Chemical, Ann Arbor, MI, USA).

2.6. Histochemical procedure

Brain cortices from 5 rats per group were extracted and processed as follows. Deeply anesthetized animals (100 mg/kg body weight i.p. ketamine, and 5 mg/kg body weight i.p. xylazine) were perfused through the left ventricle with 50 ml of carbogenated 0.01 M phosphate-buffered saline (PBS; pH 7.4), and then with 300 ml of 4% paraformaldehyde in 0.1 M phosphate buffer (PB). The brains were removed and then post-fixed for a further 4-h period in the same fixative at room temperature. Samples were then cryoprotected by immersion overnight at 4 °C in 0.1 M PB containing

30% sucrose. Afterwards, the brains were embedded in O.C.T medium and frozen in 2-methylbutane pre-chilled in liquid nitrogen. Serial rostrocaudal sections (40 μm) were cut using a cryostat (Cryocut 1800. Reichert Jung, Wetzlar, Germany). Free-floating sections were incubated for 4h in PBS containing 0.1% Triton X-100. After several washes in 0.1 M Tris-HCl, pH 7.4 buffer, the sections were incubated in the dark, for 45 min at 37 °C, in 0.1 M Tris-HCl, pH 7.4, containing 1 mM β-NADPH and 2 mM NBT (in 70% dimethylformamide). After being washed twice with 0.1 M Tris-HCl, pH 7.4, the sections were quickly dehydrated in a graded ethanol series, cleared, and mounted in DPX (Fluka, Madrid, Spain).

2.7. Thiobarbituric acid reactive substances (TBARS)

The measurement of TBARS is a good indicator of lipid peroxidation, a major marker of oxidative stress [54]. TBARS were determined spectrophotometrically following the manufacturer's recommendations (OXI-TEK TBARS assay kit, Enzo Life Sciences, Inc., Farmingdale, NY, USA). The lipid peroxidation level was expressed as nmol of malondialdehyde (MDA) formed per ml.

2.8. HIF-1α and NF-κB

Both HIF-1α (10006910, Cayman Chemical, Ann Arbor, MI, USA) and NF-κB (10007889, Cayman Chemical, Ann Arbor, MI, USA) determinations were performed on nuclear extracts (10009277, Cayman Chemical, Ann Arbor, MI, USA) following the manufacturer's recommendations. In short, Cayman's HIF-1α and NF-κB (p65) transcription factor assays are non-radioactive, sensitive method for detecting specific transcription factor DNA binding activity in nuclear extracts. Specific double stranded DNA (dsDNA) sequences containing the HIF-1α and NF-κB response elements are immobilized to the wells of 96-well plates. HIF-1α and NF-κB contained in nuclear extracts, bind specifically to the response elements. The HIF and NF-κB transcription factor complexes are detected by addition of a specific primary antibody directed against HIF-1α and NF-κB. A secondary antibody conjugated to HRP is added to provide a sensitive colorimetric readout at 450 nm.

2.9. Statistical analysis

All analyses were performed using the free-GNU R software, R version 3.2.3 (R Foundation for Statistical Computing, http://www.r-project.org/) with *car*, data.*table*, *Hmisc*, *ggplot2*, and *sm* libraries, and Wilcox' *Rallfun-v30.txt* library (http://www-rcf.usc.edu/~rwilcox/. Ask for the functions *t1wayv2*, *t2wayv2*, *mcp2atm*, *lincon*, *ESmainMCP*, *eslmcp*, and *yuenv2*). The results obtained through experiments are summarized in a Box-Plot graph according to robust statistics based on median, to which have been inserted a crossbar with the trimmed mean ± SEM. The first type of representation allows to explore the statistical assumptions, while the second type of graph allows the comparison of means, as would be done with classical statistics, but based on robust alternative statistical (trimmed mean rather than the arithmetic mean). The Box-Plot graph brings different properties of the data: A measure of location. e.g., Median-contained within a measure of dispersion (the hinge), the maximum dispersion range (the whiskers), and the possible presence of outliers (the points exceeds whiskers). The examination of experimental data (see Figs. 2, 3 and 5 to 8) shows that variability is somewhat irregular across groups (e.g. more evident in Fig. 7, where the sizes of the boxes are quite different); that is, some data did not fulfill the homocedasticity assumption. Furthermore, the presence of outliers (or observations that lies at an abnormal distance from most data) is confirmed (e.g. at least Figs. 2, 3b and 5, 7, 8a, and 8b reveal the presence of black points beyond the fences). Consequently, hereinafter we opted for robust statistical analysis, in order to protect the findings against such problems [55].

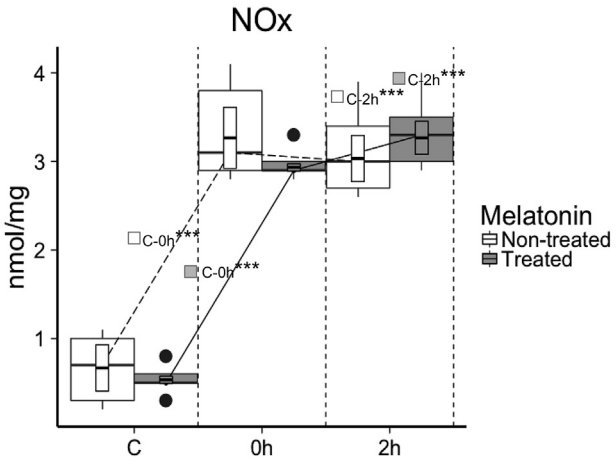

Fig. 2. NOx determination. Comparison of NOx levels of control (C, Mel + C) and experimental (0h, Mel+0h, 2h, Mel+2h) rats arranged in a 2 Melatonin x 3 IH Between Factorial Design. The results for 5 animals through 5 determinations from each group are summarized in a Box-Plot graph according to robust statistics based on median, to which a crossbar has been superimposed, showing the trimmed mean ± SEM, expressed as nmol/mg. The data exhibit some outliers (see the black points exceeding whiskers). Only comparisons that are statistically meaningful according to the significance levels (*$p \leq 0.01$, **$p \leq 0.01$, or ***$p \leq 0.001$) are highlighted with asterisks. Two-way Robust ANOVA [IH Model: $V_W = 169.293$, $p < 0.001$, Ef.Size = 0.729; Melatonin: $V_W = 0.154$, $p < 0.706$, Ef.Size = 0.018; and interaction: $V_W = 1.266$, $p < 0.601$, Ef.Size = 0.495] followed by Robust *post hoc* test of main effects [C-0h: T_W (3.856) = -10.441, $p < 0.0005$, Ef.Size = 0.950; C-2h: T_W (5.687) = -11.182, $p < 0.0000$, Ef.Size = 0.946; 0h-2h: T_W (4.997) = -0.193, $p < 0.8548$, Ef.Size = 0.291].

The six groups of rats were arranged in a 2 Melatonin (Treated vs. Non-treated) x 3 IH (Control vs. 0h vs. 2h) Between Factorial Design, to analyze the independent effect of IH Model or Melatonin, compared to the combined effect (or interaction) between the two manipulations. In all analyses, we first tested IH by melatonin interactions. If there was a significant interaction, we tested for simple effects of IH on each individual melatonin-treated group using *post hoc* multiple comparison tests that control for Type I error. When there was no significant interaction, we conducted *post hoc* tests for the main effects of the IH model. Finally, in all these analytical steps, we added the estimated effect size from Robust Wilcox [55] "Explanatory Measures". Statistical significance was set at $p \leq 0.05$. Robust analyses of variance on trimmed means (V_W) were conducted by using the method described by Wilcox [55], based on the generalization of Algina and Olejnik [56] from the Johansen [57] matrix algebra of factorial designs. Robust contrasts were conducted by a *t*-test trimmed variant (T_W), based on Yuen-Welch sequentially rejective *post hoc* test (see Ref. [55] for details).

3. Results

3.1. NO/NOS system

To ascertain melatonin treatment-related features of NO production and accumulation in the brain cortex, we made tissue measurements of total nitrogen oxides (NOx) on denatured homogenates from melatonin-treated and non-treated rats submitted to IH. The results for the NOx levels were significantly higher as a consequence of IH, independently of the administration of melatonin (Fig. 2). Hence, there were significant *post hoc* differences between C-0h ($p \leq 0.001$) and C-2h ($p \leq 0.001$) but not between 0h and 2h ($p > 0.05$) in both treated and non-treated animals.

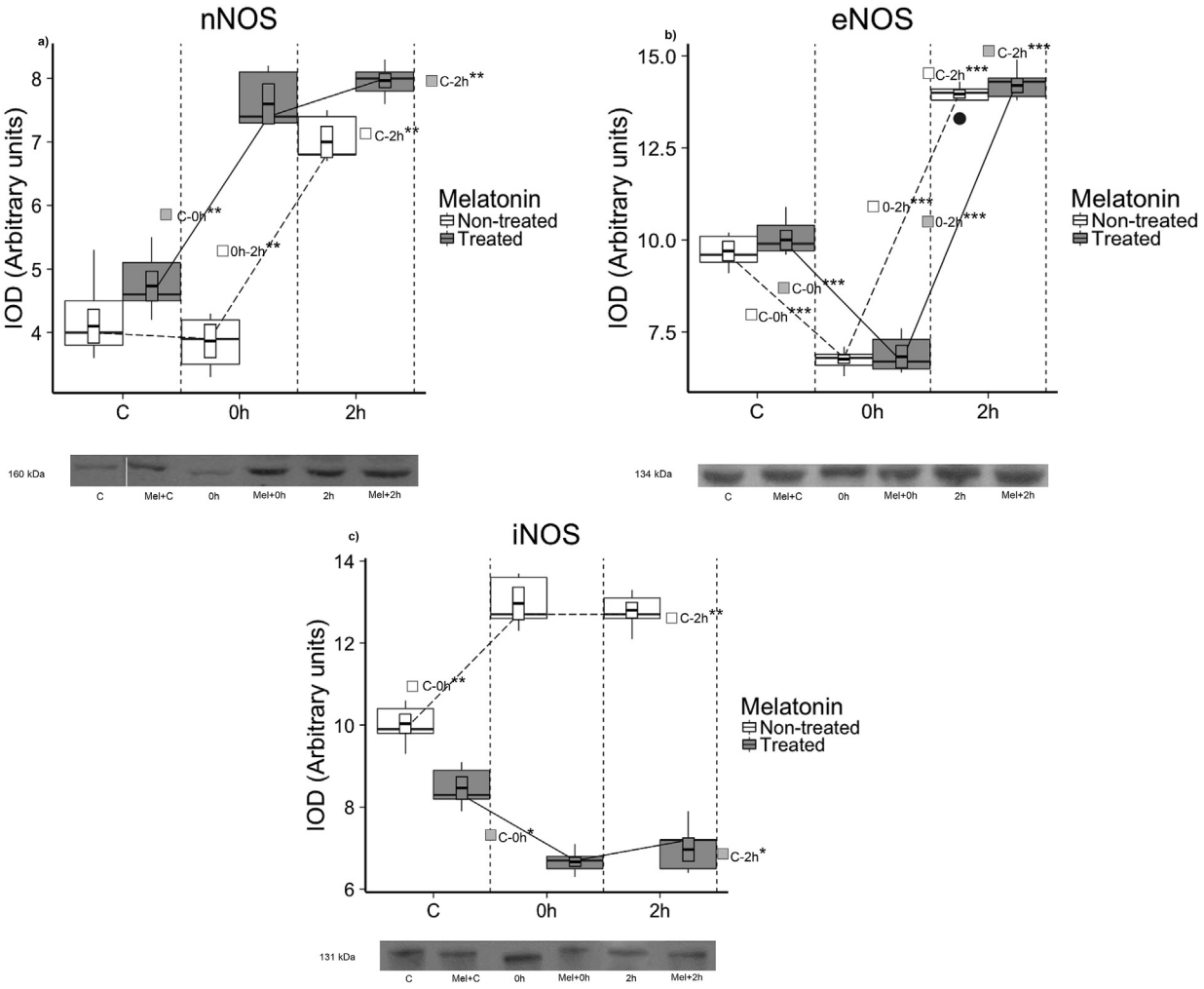

Fig. 3. Western blot analysis of **a)** nNOS, **b)** eNOS and **c)** iNOS in brain cortex cytosolic extracts of control (C, Mel + C) and experimental (0h, Mel+0h, 2h, Mel+2h) rats arranged in a 2 Melatonin x 3 IH Between Factorial Design. The amount of protein loaded per lane was 20 μg. Total protein amount of samples showed no differences between any experimental group and control; data (mean ± SEM) are expressed in mg/ml (C, 4.95 ± 0.13; Mel + C, 5.03 ± 0.14; 0h, 5.01 ± 0.12; Mel+0h, 4.87 ± 0.07; 2h, 4.90 ± 0.15; Mel+2h, 4.79 ± 0.11). Representative autoradiographies of the corresponding nNOS, eNOS and iNOS bands are displayed in the bottom panels. The results for 5 animals from each group are summarized in a Box-Plot graph according to robust statistics based on median, to which a crossbar has been superimposed, showing the trimmed mean ± SEM, expressed as arbitrary units of integrated optical density (IOD). The data exhibit some outliers (see the black points exceeding whiskers in 3b). Only comparisons that are statistically meaningful according to the significance levels ($^{*}p \leq 0.01$, $^{**}p \leq 0.01$, or $^{***}p \leq 0.001$) are highlighted with asterisks. Two-way Robust ANOVA of nNOS [IH Model: $V_W = 164.541$, $p < 0.001$, Ef.Size = 0.640; Melatonin: $V_W = 64.942$, $p < 0.001$, Ef.Size = 0.689; interaction: $V_W = 33.096$; $p < 0.001$; Ef.Size = 0.777] was followed by Robust *post hoc* test of simple effects [For the IH levels in No treated Melatonin Group, between C-0h: $T_W (3.999) = 0.572$, $p = 0.5982$, Ef.Size = 0.350; C-2h: $T_W (3.974) = 7.327$, $p < 0.0019$, Ef.Size = 0.989; and 0h-2h: $T_W (3.983) = 7.984$, $p < 0.0014$, Ef.Size = 0.981. In Melatonin Treated Group, between C-0h: $T_W (3.69) = 6.683$, $p < 0.0035$, Ef.Size = 0.974; C-2h: $T_W (2.89) = 11.384$, $p < 0.0017$, Ef.Size = 0.912; and 0h-2h: $T_W (2.508) = 1.002$, $p < 0.4031$, Ef.Size = 0.521]. Two-way Robust ANOVA of eNOS [IH Model: $V_W = 1201.442$, $p < 0.001$, Ef.Size = 0.940; Melatonin: $V_W = 1.009$, $p < 0.341$, Ef.Size = 0.064; interaction: $V_W = 0.217$, $p < 0.909$, Ef.Size = 0.203] was followed by Robust *post hoc* test of main effects [C-0h: $T_W (6.491) = 11.199$, $p < 0.000$, Ef.Size = 0.965; C-2h: $T_W (6.349) = -17.68$, $p < 0.000$, Ef.Size = 0.937, and 0h-2h: $T_W (4.676) = -33.655$, $p < 0.000$, Ef.Size = 0.919]. Two-way Robust ANOVA of iNOS [IH Model: $V_W = 6.190$, $p < 0.122$, Ef.Size = 0.115; Melatonin: $V_W = 374.382$, $p < 0.001$, Ef.Size = 0.958, and interaction: $V_W = 83.763$, $p < 0.001$, Ef.Size = 0.814] was followed by Robust *post hoc* test of simple effects [For the IH levels in No Melatonin treated Group, between C-0h: $T_W (3.240) = 5.828$, $p < 0.0081$, Ef.Size = 0.982; C-2h: $T_W (3.864) = 8.342$, $p < 0.0013$, Ef.Size = 0.961; and 0h-2h: $T_W (2.9) = 0.346$, $p < 0.7532$, Ef.Size = 0.232. In Melatonin Treated Group, between C-0h: $T_W (2.662) = 5.546$, $p < 0.0157$, Ef.Size = 0.976; C-2h: $T_W (3.993) = 3.459$, $p < 0.0259$, Ef.Size = 0.885; and 0h-2h: $T_W (2.611) = 0.891$, $p < 0.4473$, Ef.Size = 0.422].

To study the expression patterns of the NOS isoforms in the brain cortex of the rats submitted to our experimental model of IH, we performed a western blot analysis using nNOS, eNOS, and iNOS antibodies in rat-brain cortical samples (Fig. 3a, b and c). After the densitometry and analysis of the resulting bands, melatonin treated animals showed a spike in nNOS expression immediately after IH; thus, we found significant *post hoc* differences between C-0h ($p \leq 0.01$) and C-2h ($p \leq 0.01$), but not between 0h and 2h ($p > 0.05$). By contrast, non-treated rats showed a later response, peaking later after IH (2h), and thus we found non-significant *post hoc* differences between C-0h ($p > 0.0.05$) but significant differences between C-2h ($p \leq 0.01$) and between 0h and 2h, ($p \leq 0.01$) (Fig. 3a).

After IH, eNOS expression decreased in melatonin-treated and non-treated animals, reaching significant *post hoc* differences between C-0h in both groups ($p \leq 0.001$). However, after 2h of reoxygenation, eNOS expression increased both in treated and non-treated animals, showing significant *post hoc* differences between C-2h ($p \leq 0.001$) as well as between 0h and 2h ($p \leq 0.001$) (Fig. 3b).

iNOS expression showed contrasting patterns in melatonin-treated compared to non-treated rats. Thus, animals without melatonin underwent an increase after IH (0h, 2h), with significant *post hoc* differences between C-0h ($p \leq 0.01$) and C-2h ($p \leq 0.01$) but not between 0h and 2h ($p > 0.05$). Meanwhile, animals treated

with melatonin showed reduced iNOS expression, with significant *post hoc* differences between C-0h ($p \leq 0.05$) and C-2h ($p \leq 0.05$) but not between 0h and 2h, ($p > 0.05$) (Fig. 3c). Therefore, melatonin causes nNOS expression to be earlier and stronger but diminishes iNOS expressions after HI.

3.2. NADPH-diaphorase activity

After treatment with aldehydes, only NOS-related NADPH-diaphorase (NADPH-d) activity remains, so that NADPH-d histochemical staining is normally used as a complementary method for the indirect demonstration of NOS activity by light microscopy [58–60].

NADPH-d staining was clearly visualized both in the endothelium of blood vessels and in neurons. As can be seen, immediately after IH (both 0h and Mel+0h groups) no staining was detected in the vascular endothelium, being restricted to the neuronal soma and more intense in the melatonin treated animals (Mel+0h group). After the reoxygenation period the staining kept patent in neurons but reached the highest intensity at endothelial level in both groups (2h; Mel+2h) (Fig. 4a and b).

3.3. n-Tyr

Protein nitration is not an unspecific but rather a selective process that affects specific proteins, altering their activities. In this sense, tyrosine nitration has been considered to be a marker of protein degradation [61]. The western blot analysis of protein nitration detected six n-Tyr-immunoreactive (n-Tyr-IR) bands. These bands corresponded to proteins with molecular weights of 45, 42, 35, 30, 25, and 20 kDa (Fig. 5). Nevertheless, in the densitometric quantification, the total sum of nitrated proteins was considered. The Wilcox Robust ANOVAs showed that, in the absence of melatonin, protein nitration levels augmented progressively after IH at both initial reoxygenation times, showing significant *post hoc* differences between C-0h ($p \leq 0.01$) and C-2h ($p \leq 0.05$) but not between 0h and 2h ($p > 0.05$), whereas the melatonin-treated rats showed lower basal levels of protein nitration than non-treated animals at all IH levels; in fact, a significant main effect of melatonin was detected in the Robust ANOVA ($p \leq 0.001$) (Fig. 5). Thus, melatonin diminished the expression of n-Tyr after HHI.

3.4. GFAP

We analyzed the expression of the glial fibrillary acidic protein (GFAP) as a marker of glial reactivity [62] by western blot. Now, the Robust ANOVA showed significant differences only by the effect of the IH model ($p \leq 0.001$), while melatonin treatment did not influence this pattern ($p > 0.05$) or the interaction ($p > 0.05$). Specifically, our data for both non-treated and melatonin-treated animals indicated an increase in GFAP expression after IH, showing significant *post hoc* differences between all IH levels: C-0h ($p \leq 0.001$), C-2h ($p \leq 0.001$) and 0h-2h ($p \leq 0.05$) (Fig. 6). Hence, melatonin did not influence the GFAP expression after HHI.

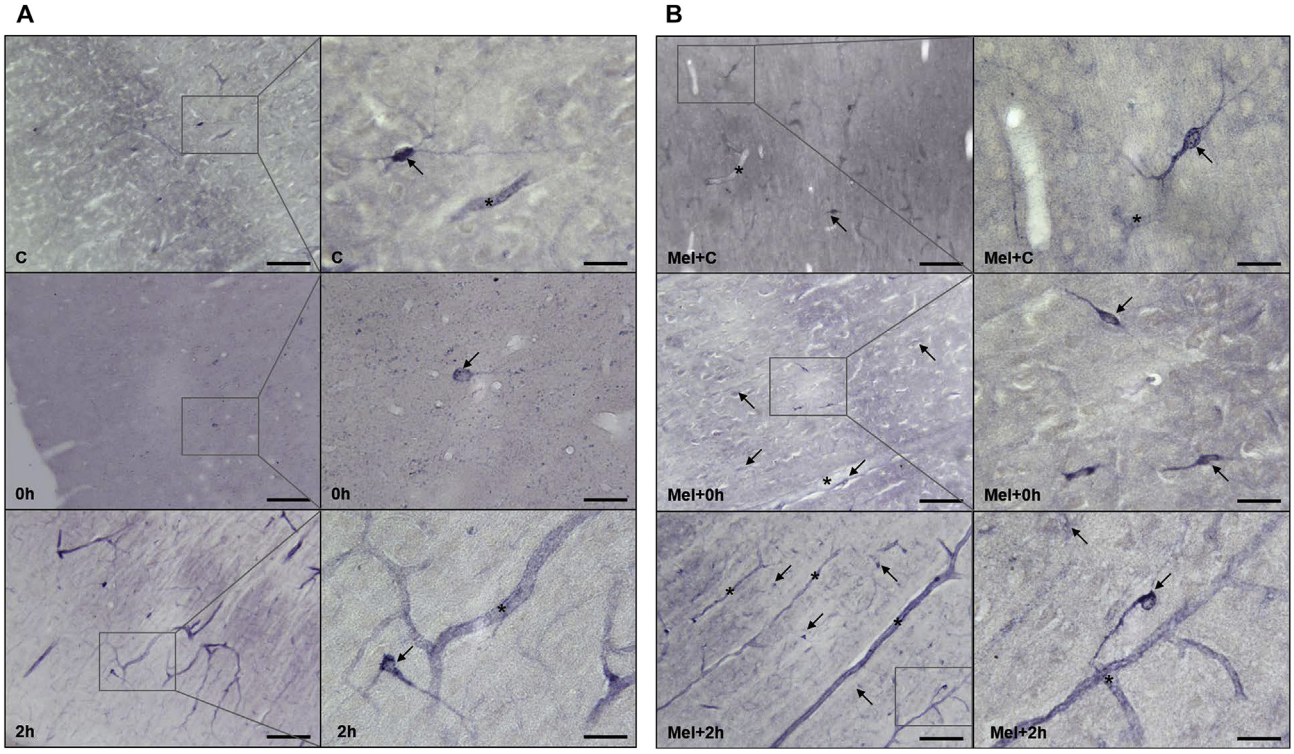

Fig. 4. Microphotographs of NADPH-diaphorase activity in rostrocaudal brain slices of control (C, Mel + C) and experimental (0h, Mel+0h, 2h, Mel+2h) rats. **a)** Non-treated animals. **b)** Treated animals. Regardless of melatonin administration, NADPH-d staining in control animals (C, Mel + C) was detected both in the endothelium of blood vessels and in neuronal soma. However, the endothelial staining faded almost completely immediately after OD (0h, Mel+0h), whereas the cellular immunostaining was restricted to scarce neuronal soma in non-treated animals (0h), but maintained or even increased in treated animals (Mel+0h). A strong mark in blood vessels after 2h of reoxygenation was observed independently of melatonin administration (2h, Mel+2h). On the other hand, a persistence of neuron staining after 2h of reoxygenation was detected in non-treated animals (2h), although increased NADPH-diaphorase neuron staining was detected in treated animals (Mel+2h). Arrows: cell soma. Asterisks: blood vessels. Scale bars: Microphotographs on the left, 100 μm; microphotographs on the right, 20 μm.

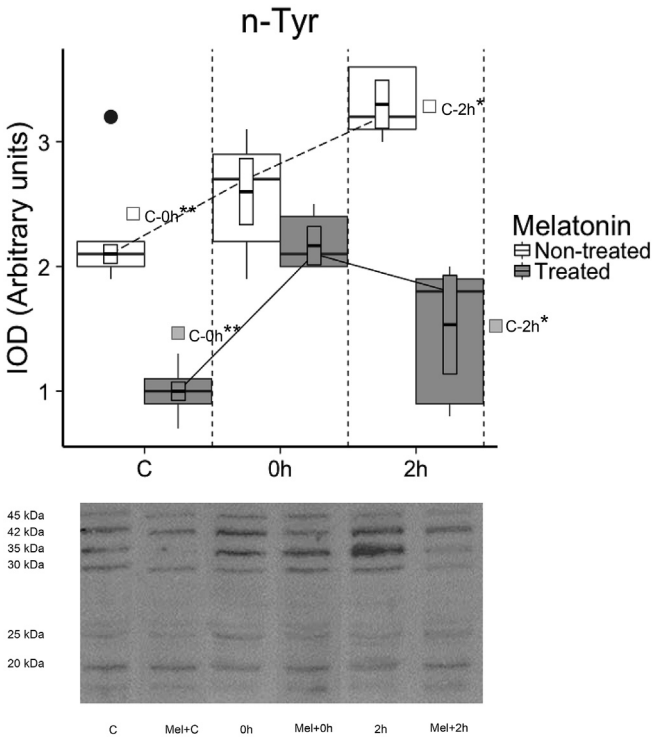

Fig. 5. Nitrated proteins study. Comparison of western blot analysis data of nitrotyrosine-modified proteins in brain-cortex cytosolic extracts of control (C, Mel + C) and experimental (0h, Mel+0h, 2h, Mel+2h) rats arranged in a 2 Melatonin x 3 IH Between Factorial Design. The amount of protein load per lane was 20 μg. Total protein amount of samples showed no differences between any experimental group and control; data (mean ± SEM) are expressed in mg/ml (C, 4.95 ± 0.13; Mel + C, 5.03 ± 0.14; 0h, 5.01 ± 0.12; Mel+0h, 4.87 ± 0.07; 2h, 4.90 ± 0.15; Mel+2h, 4.79 ± 0.11). Representative autoradiography of the corresponding n-Tyr bands is displayed in the bottom panel. The results for 5 animals from each group are summarized in a Box-Plot graph according to robust statistics based on median, to which a crossbar has been superimposed, showing the trimmed mean ± SEM, expressed as arbitrary units of integrated optical density (IOD). The data exhibit some outliers (see the black points exceeding whiskers). Only comparisons that are statistically meaningful according to the significance levels (*$p \leq 0.01$, **$p \leq 0.01$, or ***$p \leq 0.001$) are highlighted with asterisks. Two-way Robust ANOVA [IH Model: $V_W = 31.957$, $p < 0.002$, Ef.Size = 0.470; Melatonin: $V_W = 30.362$, $p < 0.001$, Ef.Size = 0.838; and interaction: $V_W = 5.749$, $p < 0.156$; Ef.Size = 0.764] followed by Robust *post hoc* test of main effects [C-0h: T_W (3.949) = -4.695, $p < 0.0096$, Ef.Size = 0.744; C-2h: T_W (3.234) = -3.495, $p < 0.0352$, Ef.Size = 0.503; 0h-2h: T_W (5.266) = -0.113, $p < 0.9139$, Ef.Size = 0.162].

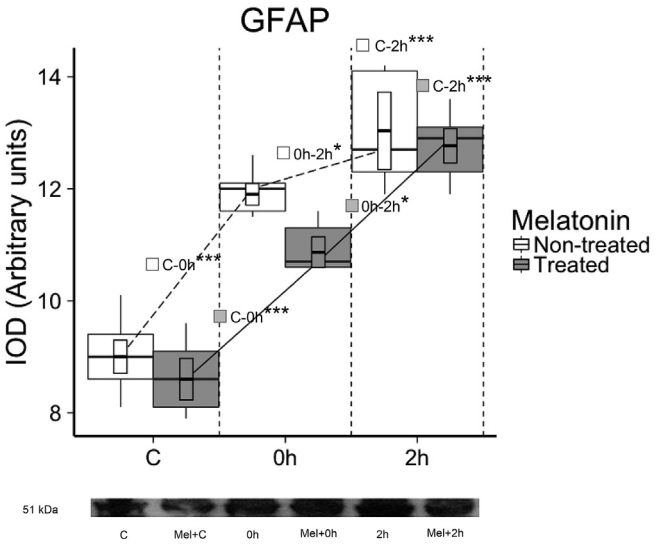

Fig. 6. Western blot analysis of GFAP in brain cortex cytosolic extracts of control (C, Mel + C) and experimental (0h, Mel+0h, 2h, Mel+2h) rats arranged in a 2 Melatonin x 3 IH Between Factorial Design. The amount of protein load per lane was 20 μg. Total protein amount of samples showed no differences between any experimental group and control; data (mean ± SEM) are expressed in mg/ml (C, 4.95 ± 0.13; Mel + C, 5.03 ± 0.14; 0h, 5.01 ± 0.12; Mel+0h, 4.87 ± 0.07; 2h, 4.90 ± 0.15; Mel+2h, 4.79 ± 0.11). Representative autoradiography of the corresponding GFAP band is displayed in the bottom panel. The results for 5 animals from each group are summarized in a Box-Plot graph according to robust statistics based on median, to which a crossbar has been superimposed, showing the trimmed mean ± SEM, expressed as arbitrary units of integrated optical density (IOD). Only comparisons that are statistically meaningful according to the significance levels (*$p \leq 0.01$, **$p \leq 0.01$, or ***$p \leq 0.001$) are highlighted with asterisks. Two-way Robust ANOVA [IH Model: $V_W = 94.381$, $p < 0.001$, Ef.Size = 0.890; Melatonin: $V_W = 2.643$, $p < 0.147$, Ef.Size = 0.208; and interaction: $V_W = 1.384$, $p < 0.566$, Ef.Size = 0.376] followed by Robust post hoc test of main effects [C-0h: T_W (6.76) = -8.089, $p < 0.0001$, Ef.Size = 0.963; C-2h: T_W (4.832) = -8.375, $p < 0.0005$, Ef.Size = 0.972; and 0h-2h: T_W (3.828) = -3.35, $p < 0.0306$, Ef.Size = 0.735].

3.5. TBARS

Regarding TBARS measures, the Wilcox Robust ANOVA showed that melatonin interacts significantly with the IH model. Specifically, the results using the TBARS assay showed a higher degree of lipid peroxidation after the ischemic damage in the non-treated animals. Thus, TBARS showed an increase after IH at 0h with significant *post hoc* differences between C-0h ($p \leq 0.001$) and C-2h ($p \leq 0.05$) but not between 0h and 2h ($p > 0.05$). The administration of melatonin maintained lower TBARS levels although it did not initially alter the rate of lipid peroxidation compared to basal levels, since an increase was seen at 0h, reaching significance between C-0h ($p \leq 0.05$). However, values dropped to basal levels at 2h and, in fact, there were no significant differences between C-2h, ($p > 0.05$) in the melatonin-treated animals (Fig. 7). Thus, as shown, melatonin protects the brain cortex from oxidation after IH.

3.6. NF-κB and HIF-1α

Both the treated and non-treated groups presented similar expression of NF-κB. However, despite the rise in NF-κB levels in the reoxygenation, after IH none of the variables analyzed reached the criterion for statistical significance: IH model ($p < 0.157$), melatonin treatment ($p < 0.186$), or interaction between IH and melatonin treatment ($p < 0.893$) (Fig. 8a).

Concerning HIF-1α levels, the Robust ANOVA showed that the only significant effect was due to IH ($p \leq 0.001$), but not to melatonin treatment ($p > 0.05$), or the interaction between both IH and melatonin ($p > 0.05$). Thus, our results showed, either in the animals treated with melatonin or in the non-treated individuals, the same pattern characterized by a decrease in the HIF-1α expression in the reoxygenation period; hence, significant *post hoc* differences were seen among all IH levels in both non-treated and treated animals: C-0h ($p \leq 0.05$), C-2h ($p \leq 0.001$), and 0h-2h ($p \leq 0.001$) (Fig. 8b).

Therefore, melatonin treatment does not alter the expression pattern of both transcriptions factors after IH. In fact, our IH model did not affect NF-κB and diminished HIF-1α nuclear expressions.

4. Discussion

A balanced NO/NOS system is crucial to maintain neuronal functionality avoiding oxidative/nitrosative damage caused by illnesses like IH and other cerebral pathologies [63]. The administration of melatonin, a potent antioxidant that is able to reduce the infarct volume after a rat model of stroke [64,65], may alleviate the neurotoxic effect of the NO reducing peroxynitrite formation and nitrosative damage [64]. Nevertheless, the mechanisms by which melatonin balances

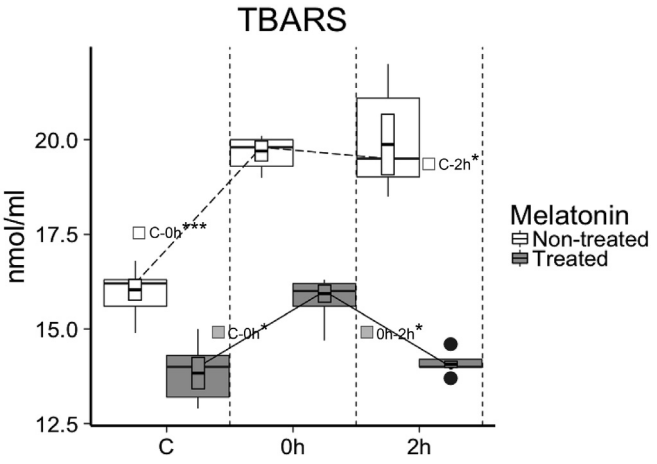

Fig. 7. TBARS study. Influence of IH on lipid peroxidation in brain cortex extracts of control (C, Mel + C) and experimental (0h, Mel+0h, 2h, Mel+2h) rats arranged in a 2 Melatonin x 3 IH Between Factorial Design. The results for 5 animals from each group through three independent experiments are summarized in a Box-Plot graph according to robust statistics based on median, to which a crossbar has been superimposed, showing the trimmed mean ± SEM, expressed as nmol of malondialdehyde (MDA) formed per ml. The data exhibit some outliers (see the black points exceeding whiskers). Only comparisons that are statistically meaningful according to the significance levels ($^{*}p \leq 0.01$, $^{**}p \leq 0.01$, or $^{***}p \leq 0.001$) are highlighted with asterisks. Two-way Robust ANOVA [IH Model: $V_W = 74.605$, $p < 0.001$, Ef.Size = 0.457; Melatonin: $V_W = 113.907$, $p < 0.001$, Ef.Size = 0.911; and interaction: $V_W = 13.002$, $p < 0.032$, Ef.Size = 0.971] followed by Robust post hoc test of simple effects [For the IH levels in No Melatonin Group, between C-0h: T_W (3.996) = 8.773, $p < 0.0009$, Ef.Size = 0.971; C-2h: T_W (2.465) = 4.158, $p < 0.0367$, Ef.Size = 0.975; and 0h-2h: T_W (2.439) = 0.188, $p < 0.8652$, Ef.Size = 0.164. In Melatonin Treated Group, between C-0h: T_W (3.076) = 4.032, $p < 0.0262$, Ef.Size = 0.841; C-2h: T_W (2.152) = 0.500, $p < 0.6637$, Ef.Size = 0.419, and between 0h and 2h: T_W (2.513) = 7.089, $p < 0.0101$, Ef.Size = 0.949].

the NO/NOS pathway are still not completely understood.

Our results indicate that melatonin positively alters the NO/NOS pathway induced by the IH model, but in different ways through the four different interrelated systems studied (NO/NOS system itself, glial reactivity, oxidative/nitrosative status of the tissue, and indirect network pathways). The study includes a robust statistical analysis; hence, the six groups of rats (C, Mel + C, 0h, Mel+0h, 2h, and Mel+2h) were arranged into a 2 melatonin (Treated vs. Non-treated) x 3 IH (Control vs. 0h vs. 2h) Between Factorial Design, which makes it possible to analyze the independent effect of IH model or melatonin treatment, compared to the combined effect (or interaction) between the two manipulations. With this preliminary assumption, we discussed our results in order to determine how melatonin interferes in the 4 interrelated systems of the NO/NOS pathway of ischemic cascade included in our study.

As previously stated, ischemic-hypoxic pathologies trigger a sequence of molecular events in which free radicals of oxygen and nitrogen play an important role [12,66]. In this sense, our model of IH provokes a strong imbalance of the NO/NOS system in the cerebral cortex, prompting a general overexpression of the three NOS isoforms as well as of NOx and n-Tyr levels after 2h of reoxygenation. In addition, we detected increases in oxidative impacts (measured as TBARS), in reactive gliosis (as augmented GFAP expression) and changes in nuclear HIF-1 expression. Melatonin treatment induced a stronger and more rapid response of nNOS expression after IH, which reached significance at 0h of reoxygenation in relation to non-treated animals. While iNOS levels rose after IH at 0h and 2h, melatonin significantly depressed its expression at both reoxygenation times. Regarding eNOS, its levels fell dramatically immediately after IH independently of melatonin administration, but rose after longer reoxygenation periods both in

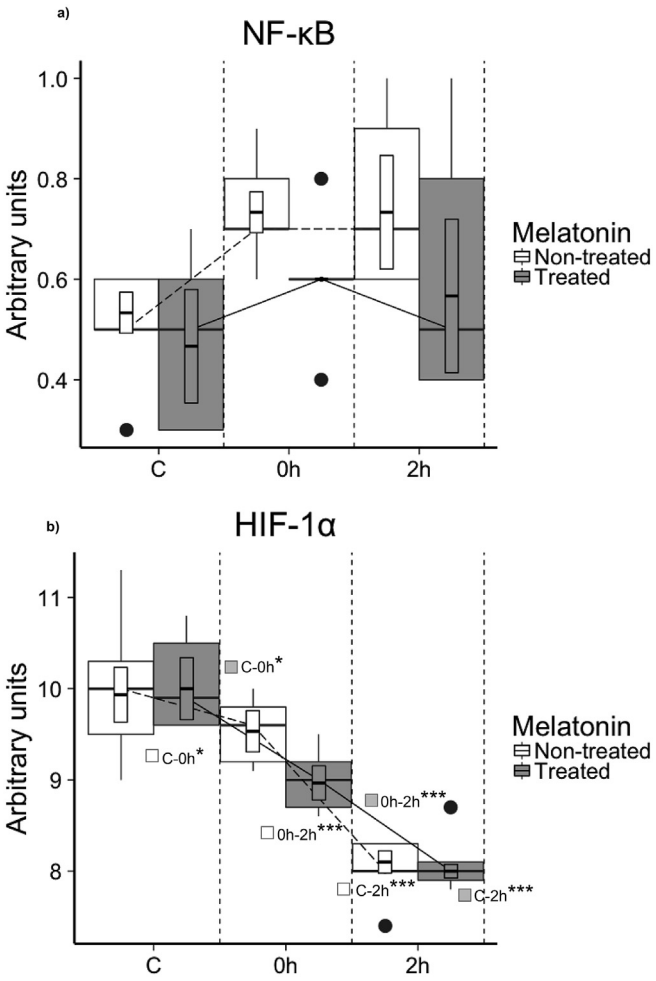

Fig. 8. a) NF-κB and **b)** HIF-1α determinations. Comparison of NF-κB and HIF-1α expression in brain cortex nuclear extracts of control (C, Mel + C) and experimental (0h, Mel+0h, 2h, Mel+2h) rats arranged in a 2 Melatonin x 3 IH Between Factorial Design. The results, which are mean values of 3 independent experiments for 5 animals from each group, are summarized in a Box-Plot graph according to robust statistics based on median, to which a crossbar has been superimposed, showing the trimmed mean ± SEM, expressed in arbitrary units. The data exhibit some outliers (see the black points exceeding whiskers). Only comparisons that are statistically meaningful according to the significance levels ($^{*}p \leq 0.01$, $^{**}p \leq 0.01$, or $^{***}p \leq 0.001$) are highlighted with asterisks. Two-way Robust ANOVA of NF-κB [IH Model: $V_W = 5.747$, $p < 0.157$, Ef.Size = 0.566; Melatonin: $V_W = 2.145$, $p < 0.186$, Ef.Size = 0.43; and interaction: $V_W = 0.266$, $p < 0.893$, Ef.Size = 0.267]. Two-way Robust ANOVA of HIF-1α [IH Model: $V_W = 87.73$, $p < 0.001$, Ef.Size = 0.907; Melatonin: $V_W = 0.963$, $p < 0.355$, Ef.Size = 0.127; and interaction: V_W= V=1.949, $p < 0.452$, Ef.Size = 0.428] was followed by Robust post hoc test of main effects [C-0h: T_W (6.736) = 2.425, $p < 0.0471$, Ef.Size = 0.869; C-2h: T_W (4.715) = 7.368, $p < 0.0009$, Ef.Size = 0.948, and between 0h and 2h: T_W (5.559) = 6.708, $p < 0.0007$, Ef.Size = 0.904].

the melatonin-treated and non-treated rats. Finally, NOx levels remained elevated after 2h of reoxygenation, whereas protein nitration dramatically diminished after the treatment with melatonin. These data suggest that the levels of NOx observed after 2h of reoxygenation in melatonin-treated animals could be consequence of the contribution of nNOS or eNOS, but not to iNOS, which would be the main factor responsible for the extremely high levels of protein nitration (2h) in the non-treated animals. Accordingly, NADPH-diaphorase results showed no endothelial staining at 0h but a strong mark in blood vessels after 2h of reoxygenation in both melatonin treated and no treated groups. In relation to neuron staining, which is illustrative of nNOS activity, given that iNOS can also be induced after hypoxia in these cells [12], we could speculate

that after melatonin treatment both nNOS and iNOS isoforms can balance the NO production in neurons, being the first upregulated and the second one downregulated.

On the other hand, these results also suggest that the effect of the overproduction of NO derived from nNOS in ischemia, which has been associated with neurotoxicity [67,68] would be arguable, since this NO-nNOS-derived has also been reported to be responsible for the neuroprotective ischemic post-conditioning in a model of brain ischemia [20]. Moreover, this viewpoint is shared by other authors [69,70], indeed suggesting a complex regulation of the neuronal isoform, in which the role of antioxidants, like melatonin, could be crucial. In this sense, an inhibitory effect of melatonin over nNOS has been proposed, related to its binding to Ca^{2+}-CaM [71]. Our results, like those reported by Huang and colaborators [36] in a hypobaric-hypoxic model, showed a faster increase in nNOS expression after melatonin treatment. In addition, melatonin does not reduce NADPHd neuronal staining, which remains intense after IH and reoxygenation. All these results highlight the complexity of the mechanisms involved in NO production, casting broader information on the role of melatonin as regulator of nNOS activity [72]. Therefore, the NO produced by nNOS could have a different fate after melatonin administration, as this antioxidant regulates NO production, whereas it lowers the levels of superoxide, thus avoiding the formation of peroxynitrite. The behavior of nNOS after melatonin treatment would also contribute to the remarkable reduction in n-Tyr expression observed in all experimental groups when compared to the corresponding situations in the absence of antioxidant.

iNOS expression is increased in several ischemic-brain models [73], as our results also document. In fact, an excessive formation of NO by iNOS may lead to peroxynitrite-induced injury [74] and may also cause cell damage through direct inhibition of mitochondrial respiratory-chain enzymes [75]. Melatonin repressed iNOS upregulation, preventing peroxynitrite damage; accordingly, during MCAO-induced brain injury, melatonin downregulated iNOS and prevented cell death [64]. Similar iNOS results were reported after melatonin administration in a model of hypobaric hypoxia [36].

Classically, eNOS has been described as the main agent responsible for the increased vasodilation under ischemic/hypoxic conditions [2]. In this sense, most authors describe NO production from eNOS as preventive of brain damage since it inhibits platelet aggregation and neuronal apoptosis and promotes collateral circulation, vasodilation, and angiogenesis [21,22]. Nevertheless, it has been also established that the formation of $ONOO^-$ in response to stress signals requires the upstream activation of eNOS [23,76]. In addition, excessive production of NO by eNOS can be harmful, as it can lead to the development of vasogenic edema and secondary brain damage [77]. Moreover, new evidence indicates that oxidative injury can induce endothelial cell damage [78] and up-regulation of eNOS expression in cerebral blood vessels [79]. Our results show a decline in eNOS expression immediately after IH but a surge after 2h of reoxygenation, regardless of the administration of melatonin. Sivakumar and collaborators [80] reported a significant increase in eNOS expression by western blot 3h after hypoxic exposure, whereas other authors have demonstrated that permanent ischemia induces aberrant expression of eNOS [23]. Thus, according to the bibliography, the pathological relevance of eNOS up-regulation in some phases of ischemia remains unclear [23]. Our results show a decline in eNOS expression immediately after IH, but a surge after 2h of reoxygenation, regardless of the administration of melatonin. In this sense, after the administration of melatonin, controversial results also appear in the literature: it has been reported that melatonin can raise the levels of eNOS protein in a model of chronic intermittent hypoxia [81], but on the other hand, melatonin can depress these levels in a model of hypobaric hypoxia [36]. Hence, it seems evident that the response of this isoform strongly depends on the hypoxic model applied in each case.

According to the above, the effect of melatonin on the NO/NOS system after IH would be due to downregulation of iNOS expression and to inhibition of nNOS activity, whose expression could be initially upregulated. Meanwhile, eNOS keeps its high levels after reoxygenation, maintaining the necessary vasodilatation. This results partially agree with others who reported nNOS and eNOS activation and iNOS inhibition as the main effects of melatonin on the NO/NOS pathway in a rat model of stroke [64].

The intermediate filaments are important in the response against cellular stress induced by glucose and oxygen deprivation [82]. Thus, astrogliosis represents greater neuroprotection, repair, and trophic supply to damaged neurons, among other benefits; the overall result of this phenomenon should be beneficial for the IH and its suppression would exacerbate tissue damage [83]. Two distinctive features of glial reactivity are hypertrophy of astrocytic processes and increased expression of intermediate filaments of GFAP [84]. Our results showed higher GFAP levels after IH injury. In addition, previous administration of melatonin did not suppress the GFAP response. Therefore, given the role of the astrocytes in the glutamate-NO-cGMP pathway, which leads to greater NO production [8], the treatment with melatonin does not affect the astrocyte contribution to the nitrosative pool, but given the ability of the antioxidant to lower the levels of oxidative stress, it may modulate its neurotoxic consequences.

Hypoxia-induced damage can also be mediated by lipid peroxidation provoked by free radicals, leading to the formation of toxic aldehydes capable of inflicting membrane de-structuring and protein carbonylation [85]. Our experimental results indicate an increase in the formation of lipid hydroperoxides in the non-treated rats at 0h and 2h after IH, while in the treated animals the levels of TBARS were clearly lowered. These results confirm melatonin cytoprotective activity due to its capacity to prevent lipid peroxidation by free-radical scavenging [32,37,86,87] and support a less $ONOO^-$ formation and consequently protein nitration found in this study.

Our results also reveal that IH injury barely affect the expression of NF-κB detected at the nuclear level during the first 2h of reoxygenation, but this pattern was not affected by melatonin, either. The role of NF-κB in brain ischemia is well characterized and may be triggered by ROS [81,88]. It participates in the inflammatory pathway, and genes coding for adhesion molecules, cytokines, and even iNOS have binding sites for this factor in their promoters. Some studies demonstrate that its inhibition has a beneficial effect, while others show that it is involved in neuronal death [89]. These contradictory results may be due to its capacity for promoting both pro-inflammatory and cell-survival factors and to its differential behavior depending on the cell type. Reportedly, melatonin may block the inflammatory process by eliminating the NF-κB signal-transduction pathway [90–92]. However, in our IH model NF-κB did not undergo expression changes, at least in the time span tested (first 2 h after hypoxia); in fact, it has been shown that the activity of this factor peaks 4–7 days after induction of ischemia [93,94]. As a result, the early iNOS changes observed after our IH model, either in the non-treated or in the melatonin-treated animals, seem to be independent of the NF-κB transcription factor in these first stages of the reoxygenation period.

Under low oxygen pressures, HIF-1α can escape prolyl-hydroxylation and subsequent proteosomal degradation; as a result, it can associate with HIF-1β and be translocated to the nucleus to induce gene expression [95]. In this light, it would be reasonable to expect higher nuclear levels of HIF-1α after IH. In this regard, although there is solid evidence that NO helps to stabilize this factor through the inhibition of prolyl-hydroxylases (PHD) [95],

it is also known that NO may exert the opposite effect, as several NO donors reduce the stabilization of HIF-1α and the transcriptional activation of downstream genes [16,96]. The latter is consistent with our results showing decreased HIF-1α expression from 0 to 2h after IH. Melatonin treatment did not influence this behavior, so that in our IH model, the capacity of melatonin to lower the levels of HIF-1α [97–99] cannot be ascribed to the antioxidant activity, at least in these first 2h after IH. In this sense, the underlying mechanisms responsible for the role on HIF-1α by melatonin are not fully understood [100], although, it has been proposed that due to scavenging of mitochondrial ROS by melatonin, the antioxidant could reverse the inactivation of PHDs by ROS. This mechanism also implies that, under hypoxia, HIF-1α would be accumulated primarily by bolstering protein stability rather than by *de novo* synthesis [97]. In any case, our model indicates that at least in the first 2h following IH, neither *de novo* synthesis nor activation of HIF-1α occurs.

5. Conclusions

This study demonstrates that after an ischemic-hypoxic event (IH), a deregulation of the NO/NOS system and related pathways occurs. Specifically, IH triggers increases in the expression of the three nitric oxide synthase (NOS) isoforms, the nitrogen oxide (NOx) levels as well as the nitrosative (n-Tyr) and oxidative (TBARS) impacts. IH also intensifies glial fibrillary acidic protein (GFAP) expression, reduces hypoxia-inducible factor-1alpha (HIF-1α), but does not change nuclear factor kappa B (NF-κB). Melatonin treatment, possibly due to its primary antioxidant capability, prevents some of these changes, not only scavenging superoxide and downregulating iNOS but also diminishing nitrosative impacts. Hence, the decrease of iNOS, besides a prompter response of the nNOS and the maintenance of the eNOS activity elicited by melatonin may contribute to balance the NO production avoiding not only the oxidative but also the nitrosative damage of these pathologies.

In addition, the results of the present study indicate that melatonin represents a suitable standard for studying and delving into the molecular mechanisms that underlie IH, as beyond its beneficial antioxidant effects, it raises questions concerning the classical role of NOS involved in the determinant first steps of the ischemic cascade, and it highlights the complexity of the equilibrium among them.

Conflict of interest

The authors declare that they have no conflict of interest.

Acknowledgments

This work was supported by the Spanish Ministry of Science and Innovation (SAF2008-03938). We thank to Mr. David Nesbitt reviewing the English language of the manuscript.

Appendix A. Supplementary data

Supplementary data related to this article can be found at http://dx.doi.org/10.1016/j.niox.2016.12.001.

References

[1] J. Rodrigo, A.P. Fernandez, J. Serrano, M.A. Peinado, A. Martinez, The role of free radicals in cerebral hypoxia and ischemia, Free Radic. Biol. Med. 39 (2005) 26–50.
[2] J.P. Bolanos, A. Almeida, Roles of nitric oxide in brain hypoxia-ischemia, Biochim. Biophys. Acta 1411 (1999) 415–436.
[3] J. Rodrigo, D. Alonso, A.P. Fernandez, J. Serrano, A. Richart, J.C. Lopez, M. Santacana, R. Martinez-Murillo, M.L. Bentura, M. Ghiglione, L.O. Uttenthal, Neuronal and inducible nitric oxide synthase expression and protein nitration in rat cerebellum after oxygen and glucose deprivation, Brain Res. 909 (2001) 20–45.
[4] M.A. Moro, A. Cardenas, O. Hurtado, J.C. Leza, I. Lizasoain, Role of nitric oxide after brain ischaemia, Cell Calcium 36 (2004) 265–275.
[5] M. Willmot, L. Gray, C. Gibson, S. Murphy, P.M. Bath, A systematic review of nitric oxide donors and L-arginine in experimental stroke; effects on infarct size and cerebral blood flow, Nitric Oxide 12 (2005) 141–149.
[6] H. Liu, J. Li, F. Zhao, H. Wang, Y. Qu, D. Mu, Nitric oxide synthase in hypoxic or ischemic brain injury, Rev. Neurosci. 26 (2015) 105–117.
[7] J.G. Wang, S.C. Bondy, L. Zhou, F.Z. Yang, Z.G. Ding, Y. Hu, Y. Tian, P.Y. Wen, H. Luo, F. Wang, W.W. Li, J. Zhou, Protective effect of Tanshinone IIA against infarct size and increased HMGB1, NFkappaB, GFAP and apoptosis consequent to transient middle cerebral artery occlusion, Neurochem. Res. 39 (2014) 295–304.
[8] R.A. Swanson, W. Ying, T.M. Kauppinen, Astrocyte influences on ischemic neuronal death, Curr. Mol. Med. 4 (2004) 193–205.
[9] C.L. Gibson, T.C. Coughlan, S.P. Murphy, Glial nitric oxide and ischemia, Glia 50 (2005) 417–426.
[10] E. Siles, E. Martinez-Lara, A. Canuelo, M. Sanchez, R. Hernandez, J.C. Lopez-Ramos, M.L. Del Moral, F.J. Esteban, S. Blanco, J.A. Pedrosa, J. Rodrigo, M.A. Peinado, Age-related changes of the nitric oxide system in the rat brain, Brain Res. 956 (2002) 385–392.
[11] R. Pannu, I. Singh, Pharmacological strategies for the regulation of inducible nitric oxide synthase: neurodegenerative versus neuroprotective mechanisms, Neurochem. Int. 49 (2006) 170–182.
[12] S. Blanco, L. Castro, R. Hernandez, M.L. Del Moral, J.A. Pedrosa, E. Martinez-Lara, E. Siles, M.A. Peinado, Age modulates the nitric oxide system response in the ischemic cerebellum, Brain Res. 1157 (2007) 66–73.
[13] V.V. Sumbayev, A. Budde, J. Zhou, B. Brune, HIF-1 alpha protein as a target for S-nitrosation, FEBS Lett. 535 (2003) 106–112.
[14] I.M. Yasinska, V.V. Sumbayev, S-nitrosation of Cys-800 of HIF-1alpha protein activates its interaction with p300 and stimulates its transcriptional activity, FEBS Lett. 549 (2003) 105–109.
[15] E. Metzen, J. Zhou, W. Jelkmann, J. Fandrey, B. Brune, Nitric oxide impairs normoxic degradation of HIF-1alpha by inhibition of prolyl hydroxylases, Mol. Biol. Cell 14 (2003) 3470–3481.
[16] U. Berchner-Pfannschmidt, S. Tug, J. Hu, B.D. Reyes, J. Fandrey, M. Kirsch, Role of N-acetyl-N-nitroso-tryptophan as nitric oxide donor in the modulation of HIF-1-dependent signaling, Biol. Chem. 391 (2010) 533–540.
[17] J.C. LaManna, J.C. Chavez, P. Pichiule, Structural and functional adaptation to hypoxia in the rat brain, J. Exp. Biol. 207 (2004) 3163–3169.
[18] I. Lizasoain, M.A. Moro, Simultaneous measurement of mitochondrial function and NO, Methods Mol. Biol. 100 (1998) 273–279.
[19] P. Pacher, J.S. Beckman, L. Liaudet, Nitric oxide and peroxynitrite in health and disease, Physiol. Rev. 87 (2007) 315–424.
[20] D. Zhang, C. Li, J. Zhou, Y. Song, X. Fang, J. Ou, J. Li, C. Bai, Autophagy protects against ischemia/reperfusion-induced lung injury through alleviating blood-air barrier damage, J. Heart Lung Transpl. 34 (2015) 746–755.
[21] C. Iadecola, Bright and dark sides of nitric oxide in ischemic brain injury, Trends Neurosci. 20 (1997) 132–139.
[22] P.L. Huang, Nitric oxide and cerebral ischemic preconditioning, Cell Calcium 36 (2004) 323–329.
[23] F. Han, Y. Shirasaki, K. Fukunaga, Microsphere embolism-induced endothelial nitric oxide synthase expression mediates disruption of the blood-brain barrier in rat brain, J. Neurochem. 99 (2006) 97–106.
[24] W.H. Koppenol, J.J. Moreno, W.A. Pryor, H. Ischiropoulos, J.S. Beckman, Peroxynitrite, a cloaked oxidant formed by nitric oxide and superoxide, Chem. Res. Toxicol. 5 (1992) 834–842.
[25] W.A. Pryor, G.L. Squadrito, The chemistry of peroxynitrite: a product from the reaction of nitric oxide with superoxide, Am. J. Physiol. 268 (1995) L699–L722.
[26] J.W. Thompson, S.V. Narayanan, M.A. Perez-Pinzon, Redox signaling pathways involved in neuronal ischemic preconditioning, Curr. Neuropharmacol. 10 (2012) 354–369.
[27] K. Jian Liu, G.A. Rosenberg, Matrix metalloproteinases and free radicals in cerebral ischemia, Free Radic. Biol. Med. 39 (2005) 71–80.
[28] R.A. Dweik, Nitric oxide, hypoxia, and superoxide: the good, the bad, and the ugly!, Thorax 60 (2005) 265–267.
[29] C. Charriaut-Marlangue, P. Bonnin, P.L. Leger, S. Renolleau, Brief update on hemodynamic responses in animal models of neonatal stroke and hypoxia-ischemia, Exp. Neurol. 248 (2013) 316–320.
[30] A. Galano, D.X. Tan, R.J. Reiter, Melatonin as a natural ally against oxidative stress: a physicochemical examination, J. Pineal Res. 51 (2011) 1–16.
[31] J.W. Jang, J.K. Lee, M.C. Lee, M.S. Piao, S.H. Kim, H.S. Kim, Melatonin reduced the elevated matrix metalloproteinase-9 level in a rat photothrombotic stroke model, J. Neurol. Sci. 323 (2012) 221–227.
[32] R.J. Reiter, J.C. Mayo, D.X. Tan, R.M. Sainz, M. Alatorre-Jimenez, L. Qin, Melatonin as an antioxidant: under promises but over delivers, J. Pineal Res. 61 (2016) 253–278.
[33] R.J. Reiter, D.X. Tan, W.B. Qi, Suppression of oxygen toxicity by melatonin, Zhongguo Yao Li Xue Bao 19 (1998) 575–581.
[34] F. Tutunculer, S. Eskiocak, U.N. Basaran, G. Ekuklu, S. Ayvaz, U. Vatansever,

The protective role of melatonin in experimental hypoxic brain damage, Pediatr. Int. 47 (2005) 434–439.
[35] M. Cervantes, G. Morali, G. Letechipia-Vallejo, Melatonin and ischemia-reperfusion injury of the brain, J. Pineal Res. 45 (2008) 1–7.
[36] C.C. Huang, C.J. Lai, M.H. Tsai, Y.C. Wu, K.T. Chen, M.J. Jou, P.I. Fu, C.H. Wu, I.H. Wei, Effects of melatonin on the nitric oxide system and protein nitration in the hypobaric hypoxic rat hippocampus, BMC Neurosci. 16 (2015) 61.
[37] G. Escames, J.M. Guerrero, R.J. Reiter, J.J. Garcia, A. Munoz-Hoyos, G.G. Ortiz, C.S. Oh, Melatonin and vitamin E limit nitric oxide-induced lipid peroxidation in rat brain homogenates, Neurosci. Lett. 230 (1997) 147–150.
[38] T. Kondoh, H. Uneyama, H. Nishino, K. Torii, Melatonin reduces cerebral edema formation caused by transient forebrain ischemia in rats, Life Sci. 72 (2002) 583–590.
[39] R. Das, L. Balonan, H.J. Ballard, S. Ho, Chronic hypoxia inhibits the antihypertensive effect of melatonin on pulmonary artery, Int. J. Cardiol. 126 (2008) 340–345.
[40] H.M. Chang, U.I. Wu, C.T. Lan, Melatonin preserves longevity protein (sirtuin 1) expression in the hippocampus of total sleep-deprived rats, J. Pineal Res. 47 (2009) 211–220.
[41] D. Maresova, V. Riljak, J. Mares, Melatonin modulates hypoxia-induced changes of rat brain excitability, Gen. Physiol. Biophys. 29 (2010) 67–71.
[42] I. Pekarkova, S. Parara, V. Holecek, P. Stopka, L. Trefil, J. Racek, R. Rokyta, Does exogenous melatonin influence the free radicals metabolism and pain sensation in rat? Physiol. Res. 50 (2001) 595–602.
[43] F. Adhami, G. Liao, Y.M. Morozov, A. Schloemer, V.J. Schmithorst, J.N. Lorenz, R.S. Dunn, C.V. Vorhees, M. Wills-Karp, J.L. Degen, R.J. Davis, N. Mizushima, P. Rakic, B.J. Dardzinski, S.K. Holland, F.R. Sharp, C.Y. Kuan, Cerebral ischemia-hypoxia induces intravascular coagulation and autophagy, Am. J. Pathol. 169 (2006) 566–583.
[44] S. Levine, Anoxic-ischemic encephalopathy in rats, Am. J. Pathol. 36 (1960) 1–17.
[45] J.E. Rice 3rd, R.C. Vannucci, J.B. Brierley, The influence of immaturity on hypoxic-ischemic brain damage in the rat, Ann. Neurol. 9 (1981) 131–141.
[46] A. Basu, J. Lazovic, J.K. Krady, D.T. Mauger, R.P. Rothstein, M.B. Smith, S.W. Levison, Interleukin-1 and the interleukin-1 type 1 receptor are essential for the progressive neurodegeneration that ensues subsequent to a mild hypoxic/ischemic injury, J. Cereb. Blood Flow. Metab. 25 (2005) 17–29.
[47] S.J. Vannucci, L.B. Willing, S. Goto, N.J. Alkayed, R.M. Brucklacher, T.L. Wood, J. Towfighi, P.D. Hurn, I.A. Simpson, Experimental stroke in the female diabetic, db/db, mouse, J. Cereb. Blood Flow. Metab. 21 (2001) 52–60.
[48] M.A. Peinado, R. Hernandez, J. Peragon, D. Ovelleiro, J.A. Pedrosa, S. Blanco, Proteomic characterization of nitrated cell targets after hypobaric hypoxia and reoxygenation in rat brain, J. Proteom. 109 (2014) 309–321.
[49] R. Hernandez, S. Blanco, J. Peragon, J.A. Pedrosa, M.A. Peinado, Hypobaric hypoxia and reoxygenation induce proteomic profile changes in the rat brain cortex, Neuromolecular Med. 15 (2013) 82–94.
[50] M.M. Bradford, A rapid and sensitive method for the quantitation of microgram quantities of protein utilizing the principle of protein-dye binding, Anal. Biochem. 72 (1976) 248–254.
[51] U.K. Laemmli, Cleavage of structural proteins during the assembly of the head of bacteriophage T4, Nature 227 (1970) 680–685.
[52] S. Blanco, F.J. Molina, L. Castro, M.L. Del Moral, R. Hernandez, A. Jimenez, A. Rus, E. Martinez-Lara, E. Siles, M.A. Peinado, Study of the nitric oxide system in the rat cerebellum during aging, BMC Neurosci. 11 (2010) 78.
[53] T. Genade, D.M. Lang, Resveratrol extends lifespan and preserves glia but not neurons of the Nothobranchius guentheri optic tectum, Exp. Gerontol. 48 (2013) 202–212.
[54] G. Lefevre, M. Beljean-Leymarie, F. Beyerle, D. Bonnefont-Rousselot, J.P. Cristol, P. Therond, J. Torreilles, Evaluation of lipid peroxidation by measuring thiobarbituric acid reactive substances, Ann. Biol. Clin. Paris. 56 (1998) 305–319.
[55] R.R. Wilcox, Introduction to Robust Estimation and Hypothesis Testing, Academic Press, San Diego, CA, 2012.
[56] J. Algina, S.F. Olejnik, Implementing the Welch-James procedure with factorial designs, Educ. Psychol. Meas. 44 (1984) 39–48.
[57] S. Johansen, The Welch-James approximation of the distribution of the residual sum of squares in weighted linear regression, Biometrika 67 (1980) 85–92.
[58] C.G. Coburn, A. Watson-Siriboe, B. Hou, C. Cheetham, E.R. Gillard, L. Lin, M. Leon-Olea, E. Sanchez-Islas, S. Mucio-Ramirez, M.C. Curras-Collazo, Permanently compromised NADPH-diaphorase activity within the osmotically activated supraoptic nucleus after in utero but not adult exposure to Aroclor 1254, Neurotoxicology 47 (2015) 37–46.
[59] N. Liman, E. Alan, Region-specific localization of NOS isoforms and NADPH-diaphorase activity in the intratesticular and excurrent duct systems of adult domestic cats (Felis catus), Microsc. Res. Tech. 79 (2016) 192–208.
[60] E. Roufail, M. Stringer, S. Rees, Nitric oxide synthase immunoreactivity and NADPH diaphorase staining are co-localised in neurons closely associated with the vasculature in rat and human retina, Brain Res. 684 (1995) 36–46.
[61] A. Castegna, V. Thongboonkerd, J.B. Klein, B. Lynn, W.R. Markesbery, D.A. Butterfield, Proteomic identification of nitrated proteins in Alzheimer's disease brain, J. Neurochem. 85 (2003) 1394–1401.
[62] S. Brahmachari, Y.K. Fung, K. Pahan, Induction of glial fibrillary acidic protein expression in astrocytes by nitric oxide, J. Neurosci. 26 (2006) 4930–4939.
[63] N.N. Nassar, R.M. Abdelsalam, A.A. Abdel-Rahman, D.M. Abdallah, Possible involvement of oxidative stress and inflammatory mediators in the protective effects of the early preconditioning window against transient global ischemia in rats, Neurochem. Res. 37 (2012) 614–621.
[64] P.O. Koh, Melatonin regulates nitric oxide synthase expression in ischemic brain injury, J. Vet. Med. Sci. 70 (2008) 747–750.
[65] Z. Pei, P.C. Fung, R.T. Cheung, Melatonin reduces nitric oxide level during ischemia but not blood-brain barrier breakdown during reperfusion in a rat middle cerebral artery occlusion stroke model, J. Pineal Res. 34 (2003) 110–118.
[66] M. Oechmichen, C. Meissner, Cerebral hypoxia and ischemia: the forensic point of view: a review, J. Forensic Sci. 51 (2006) 880–887.
[67] O.P. Mishra, R. Mishra, Q.M. Ashraf, M. Delivoria-Papadopoulos, Nitric oxide-mediated mechanism of neuronal nitric oxide synthase and inducible nitric oxide synthase expression during hypoxia in the cerebral cortex of newborn piglets, Neuroscience 140 (2006) 857–863.
[68] S.R. Parathath, I. Gravanis, S.E. Tsirka, Nitric oxide synthase isoforms undertake unique roles during excitotoxicity, Stroke 38 (2007) 1938–1945.
[69] K. Nandagopal, T.M. Dawson, V.L. Dawson, Critical role for nitric oxide signaling in cardiac and neuronal ischemic preconditioning and tolerance, J. Pharmacol. Exp. Ther. 297 (2001) 474–478.
[70] R.F. Feng, Y.Y. Hu, W.B. Li, H.Q. Liu, Q.J. Li, M. Zhang, The role of NO resulted from neuronal nitric oxide synthase in the metabotropic glutamate receptor2/3 mediated-brain ischemic tolerance, Zhongguo Ying Yong Sheng Li Xue Za Zhi 25 (2009) 182–185.
[71] J. Leon, G. Escames, M.I. Rodriguez, L.C. Lopez, V. Tapias, A. Entrena, E. Camacho, M.D. Carrion, M.A. Gallo, A. Espinosa, D.X. Tan, R.J. Reiter, D. Acuna-Castroviejo, Inhibition of neuronal nitric oxide synthase activity by N1-acetyl-5-methoxykynuramine, a brain metabolite of melatonin, J. Neurochem. 98 (2006) 2023–2033.
[72] S. Cuzzocrea, G. Costantino, E. Gitto, E. Mazzon, F. Fulia, I. Serraino, S. Cordaro, I. Barberi, A. De Sarro, A.P. Caputi, Protective effects of melatonin in ischemic brain injury, J. Pineal Res. 29 (2000) 217–227.
[73] D. Wei, X. Xiong, H. Zhao, Tim-3 cell signaling and iNOS are involved in the protective effects of ischemic postconditioning against focal ischemia in rats, Metab. Brain Dis. 36 (2015) 483–490.
[74] C. Thiemermann, H. Ruetten, C.C. Wu, J.R. Vane, The multiple organ dysfunction syndrome caused by endotoxin in the rat: attenuation of liver dysfunction by inhibitors of nitric oxide synthase, Br. J. Pharmacol. 116 (1995) 2845–2851.
[75] G.C. Brown, V. Borutaite, Inhibition of mitochondrial respiratory complex I by nitric oxide, peroxynitrite and S-nitrosothiols, Biochim. Biophys. Acta 1658 (2004) 44–49.
[76] B.M. Mitchell, L.G. Cook, S. Danchuk, J.B. Puschett, Uncoupled endothelial nitric oxide synthase and oxidative stress in a rat model of pregnancy-induced hypertension, Am. J. Hypertens. 20 (2007) 1297–1304.
[77] V.E. Thiel, K.L. Audus, Nitric oxide and blood-brain barrier integrity, Antioxid. Redox Signal 3 (2001) 273–278.
[78] Y.B. Choi, Y.I. Kim, K.S. Lee, B.S. Kim, D.J. Kim, Protective effect of epigallocatechin gallate on brain damage after transient middle cerebral artery occlusion in rats, Brain Res. 1019 (2004) 47–54.
[79] R. Veltkamp, N. Rajapakse, G. Robins, M. Puskar, K. Shimizu, D. Busija, Transient focal ischemia increases endothelial nitric oxide synthase in cerebral blood vessels, Stroke 33 (2002) 2704–2710.
[80] V. Sivakumar, J. Lu, E.A. Ling, C. Kaur, Vascular endothelial growth factor and nitric oxide production in response to hypoxia in the choroid plexus in neonatal brain, Brain Pathol. 18 (2008) 71–85.
[81] M.W. Hung, G.M. Kravtsov, C.F. Lau, A.M. Poon, G.L. Tipoe, M.L. Fung, Melatonin ameliorates endothelial dysfunction, vascular inflammation, and systemic hypertension in rats with chronic intermittent hypoxia, J. Pineal Res. 55 (2013) 247–256.
[82] Y. de Pablo, M. Nilsson, M. Pekna, M. Pekny, Intermediate filaments are important for astrocyte response to oxidative stress induced by oxygen-glucose deprivation and reperfusion, Histochem Cell Biol. 140 (2013) 81–91.
[83] A. Verkhratsky, J.J. Rodriguez, V. Parpura, Astroglia in neurological diseases, Future Neurol. 8 (2013) 149–158.
[84] M.T. Wunderlich, C.W. Wallesch, M. Goertler, Release of glial fibrillary acidic protein is related to the neurovascular status in acute ischemic stroke, Eur. J. Neurol. 13 (2006) 1118–1123.
[85] K.S. Fritz, D.R. Petersen, Exploring the biology of lipid peroxidation-derived protein carbonylation, Chem. Res. Toxicol. 24 (2011) 1411–1419.
[86] K.G. Akbulut, B. Gonul, H. Akbulut, Exogenous melatonin decreases age-induced lipid peroxidation in the brain, Brain Res. 1238 (2008) 31–35.
[87] Zamorskii II, I.Y. Sopova, V. Khavinson, Effects of melatonin and epithalamin on the content of protein and lipid peroxidation products in rat cortex and hippocampus under conditions of acute hypoxia, Bull. Exp. Biol. Med. 154 (2012) 51–53.
[88] M. Zeng, X. Wei, Z. Wu, W. Li, B. Li, Y. Zhen, J. Chen, P. Wang, Y. Fei, NF-kappaB-mediated induction of autophagy in cardiac ischemia/reperfusion injury, Biochem. Biophys. Res. Commun. 436 (2013) 180–185.
[89] C.R. Lenihan, C.T. Taylor, The impact of hypoxia on cell death pathways, Biochem. Soc. Trans. 41 (2013) 657–663.
[90] M. Alonso, P.S. Collado, J. Gonzalez-Gallego, Melatonin inhibits the expression of the inducible isoform of nitric oxide synthase and nuclear factor kappa B activation in rat skeletal muscle, J. Pineal Res. 41 (2006) 8–14.
[91] N. Mohan, K. Sadeghi, R.J. Reiter, M.L. Meltz, The neurohormone melatonin

inhibits cytokine, mitogen and ionizing radiation induced NF-kappa B, Biochem. Mol. Biol. Int. 37 (1995) 1063–1070.
[92] J.I. Chuang, N. Mohan, M.L. Meltz, R.J. Reiter, Effect of melatonin on NF-kappa-B DNA-binding activity in the rat spleen, Cell Biol. Int. 20 (1996) 687–692.
[93] H. Seegers, E. Grillon, Y. Trioullier, A. Vath, J.M. Verna, D. Blum, Nuclear factor-kappa B activation in permanent intraluminal focal cerebral ischemia in the rat, Neurosci. Lett. 288 (2000) 241–245.
[94] C. Gabriel, C. Justicia, A. Camins, A.M. Planas, Activation of nuclear factor-kappaB in the rat brain after transient focal ischemia, Brain Res. Mol. Brain Res. 65 (1999) 61–69.
[95] S.N. Greer, J.L. Metcalf, Y. Wang, M. Ohh, The updated biology of hypoxia-inducible factor, EMBO J. 31 (2012) 2448–2460.
[96] L.E. Huang, W.G. Willmore, J. Gu, M.A. Goldberg, H.F. Bunn, Inhibition of hypoxia-inducible factor 1 activation by carbon monoxide and nitric oxide. Implications for oxygen sensing and signaling, J. Biol. Chem. 274 (1999) 9038–9044.
[97] S.Y. Park, W.J. Jang, E.Y. Yi, J.Y. Jang, Y. Jung, J.W. Jeong, Y.J. Kim, Melatonin suppresses tumor angiogenesis by inhibiting HIF-1alpha stabilization under hypoxia, J. Pineal Res. 48 (2010) 178–184.
[98] S.W. Park, H.S. Lee, M.S. Sung, S.J. Kim, The effect of melatonin on retinal ganglion cell survival in ischemic retina, Chonnam Med. J. 48 (2012) 116–122.
[99] D. Lanoix, A.A. Lacasse, R.J. Reiter, C. Vaillancourt, Melatonin: the watchdog of villous trophoblast homeostasis against hypoxia/reoxygenation-induced oxidative stress and apoptosis, Mol. Cell Endocrinol. 381 (2013) 35–45.
[100] S.Y. Cho, H.J. Lee, S.J. Jeong, H.J. Lee, H.S. Kim, C.Y. Chen, E.O. Lee, S.H. Kim, Sphingosine kinase 1 pathway is involved in melatonin-induced HIF-1alpha inactivation in hypoxic PC-3 prostate cancer cells, J. Pineal Res. 51 (2011) 87–93.